Published in final edited form as:
Sci Signal. ; 7(343): ra89. doi:10.1126/scisignal.2005392.

*The autoinhibitory C-terminal SH2 domain of phospholipase C–γ2 stabilizes B cell receptor signalosome assembly

Jing Wang[1,*], **Haewon Sohn**[1,*], **Guangping Sun**[2], **Joshua D. Milner**[2], and **Susan K. Pierce**[1,†]

[1]Laboratory of Immunogenetics, National Institute of Allergy and Infectious Diseases, National, Institutes of Health, Rockville, MD 20852, USA

[2]Laboratory of Allergic Diseases, National, Institute of Allergy and Infectious Diseases, National Institutes of Health, Bethesda, MD 20892, USA

Abstract

The binding of antigen to the B cell receptor (BCR) stimulates the assembly of a signaling complex (signalosome) composed initially of the kinases Lyn, spleen tyrosine kinase (Syk), and Bruton's tyrosine kinase (Btk), as well as the adaptor protein B cell linker (BLNK). Together, these proteins recruit and activate phospholipase C–γ2 (PLC-γ2), a critical effector that stimulates increases in intracellular Ca^{2+} and activates various signaling pathways downstream of the BCR. Individuals with one copy of a mutant *PLCG2* gene, which encodes a variant PLC-γ2 that lacks the autoinhibitory C-terminal Src homology 2 (cSH2) domain, exhibit PLC-γ2– associated antibody deficiencies and immune dysregulation (PLAID). Paradoxically, although COS-7 cells expressing the variant PLC-γ2 show enhanced basal and stimulated PLC-γ2 activity, B cells from PLAID patients show defective intracellular Ca^{2+} responses upon crosslinking of the BCR. We found that the cSH2 domain of PLC-γ2 played a critical role in stabilizing the early signaling complex that is stimulated by BCR crosslinking. In the presence of the variant PLC-γ2, Syk, Btk, and BLNK were only weakly phosphorylated and failed to stably associate with the BCR. Thus, BCRs could not form stable clusters, resulting in dysregulation of downstream signaling and trafficking of the BCR. Thus, the cSH2 domain functions not only to inhibit the active site of PLC-γ2, but also to directly or indirectly stabilize the early BCR signaling complex.

†Corresponding author. spierce@nih.gov.
*These authors contributed equally to this work.

Supplementary Materials

Fig. S1. Less BCRs traffic into the HLA-DM^+ class II–processing compartment upon BCR crosslinking in PLAID B cells than in HC donor B cells.
Movies S1 to S3

Author contributions: J.W. and H.W.S. designed the study, performed the experiments, analyzed the data, and wrote the manuscript; G.S. and J.D.M. provided patient samples, critically evaluated the data, and edited the manuscript; S.K.P. conceived the project, supervised the experiments, and wrote the manuscript; and all authors read and approved the final version of the manuscript.
Competing interests: The authors declare that they have no competing interests.

Introduction

A critical effector molecule in the antigen-stimulated, B cell receptor (BCR)-dependent activation of B cells is phospholipase C–γ2 (PLC-γ2) (1). When activated, PLC-γ2 catalyzes the hydrolysis of phosphatidylinositol (4,5) bisphosphate [PI(4,5)P_2] in the plasma membrane, producing increased concentrations of cytosolic inositol 1,4,5 trisphosphate (IP_3), which acts to increase the concentration of intracellular Ca^{2+}, and of diacylglycerol (DAG), which activates various protein kinase C (PKC) isoforms (2). Together, Ca^{2+} influx and activated PKC stimulate a number of signaling pathways that lead to the expression of various genes associated with B cell activation (3). PLC-γ2 also decreases the local concentration of PI(4,5)P_2 in the plasma membrane, which affects the activities and distribution of many regulatory and structural proteins, including the actin cytoskeleton (4, 5). Thus, PLC-γ2 plays a pivotal role in determining the outcome of engagement of the BCR with antigen. Indeed, impaired Ca^{2+} signaling in B cells is linked to various immunodeficiencies and autoimmune diseases (6).

PLC-γ2 is a member of one of six PLC families that consists of itself and PLC-γ1 (2). PLC-γ1 and PLC-γ2 are complex, multidomain proteins, and we are just beginning to understand the inter- and intra-molecular interactions of these domains and how such interactions serve to regulate the activities of both isoforms (7). Similar to members of other PLC families, PLC-γ1 and PLC-γ2 consist of a core containing an N-terminal pleckstrin homology (PH) domain, an EF hands domain, a split triosephosphate isomerase (TIM)-barrel catalytic domain, which is composed of an X and a Y domain and a C2 domain. The family of PLC-γ1 and PLC-γ2 is unique in that the X and Y domains that form the TIM-barrel catalytic domain are separated by a large multi-domain insert, termed the PLC-γ–specific array (γ-SA)(8). The γ-SA is a highly structured region that includes a split PH domain, which is composed of residues at either end of the insert that fold into a structural PH domain. The loop that emerges from the split PH domain contains N-terminal Src homology 2 (nSH2) and C-terminal SH2 (cSH2) domains, as well as an SH3 domain (9). The cSH2 domain interacts with the surface of the PLC-γ core above the active site, masking and inactivating the enzyme (10). Phosphorylation of Tyr^{783} in PLC-γ1 or Tyr^{759} in PLC-γ2 in the linker region between the cSH2 domain and the SH3 domain prevents this interaction, which enables the active site of the kinase domain in the core to gain access to the membrane substrate PI(4,5)P_2 (9).

Upon BCR crosslinking, PLC-γ is recruited to the plasma membrane (1), where it forms a complex with the phosphorylated cytoplasmic domains of the immunoglobulin α (Igα) and Igβ subunits of the BCR, the membrane-tethered Src family kinase Lyn (11), phosphorylated spleen tyrosine kinase (Syk) (12), the phosphorylated adaptor protein B-cell linker (BLNK) (13–15), and activated Bruton's tyrosine kinase (Btk) (16–18). In the complex, PLC-γ2 docks on BLNK through its nSH2 domain (19, 20), and is activated by phosphorylation by Btk. Evidence indicates that PLC-γ2 also interacts with phosphorylated BLNK through its core C2 domain , which further stabilizes the association of PLC-γ2 with BLNK in a Ca^{2+} -dependent fashion (21).

Through an extensive series of experiments, Weber *et al*. (22) described the role of PLC-γ2 in the initiation and propagation of B cell signaling in response to membrane-bound antigens. These authors had previously established that when placed on an antigen-containing membrane, B cells first spread over the membrane and form signaling-active BCR microsignalosomes before contracting to form an immunological synapse (23). With this system, the authors demonstrated that PLC-γ2 is actively recruited to and functions in the BCR microsignalosomes by a mechanism that is dependent on the SH2 domains and the lipase activity of PLC-γ2, as well as on BLNK and Btk (22). Thus, the coordination of BCR-induced cell-spreading is critically dependent on the assembly of complex PLC-γ2–containing microsignalosomes.

A critical step in the regulation of B cell signaling is the unmasking of the active site of PLC-γ2, as evidenced by the observation that most mutations in PLC-γ that are associated with immune disorders in humans and mice involve B cell dysregulation and map to the cSH2 domain or to the surface of the core above the active site to which the cSH2 domain binds (10, 24–27). A study showed that in-frame deletions within the region encoding the cSH2 domain of PLC-γ2 result in antibody deficiencies, susceptibility to infections, cold urticarial, and autoimmunity in affected individuals, which is termed PLAID for PLC-γ2–associated antibody deficiency and immune dysregulation (26). In that study, B cells expressing two different PLC-γ2 deletion variants were analyzed. The first, Δ20–22, is devoid of part of the C terminus of the cSH2 domain, the linker region, and the N-terminal portion of the SH3 domain of the γ-SA (amino acid residues 686 to 806). The second deletion variant, Δ19, is devoid of only the N-terminal region of the cSH2 domain (residues 646 to 685). The region of the cSH2 domain deleted in the Δ19 variant, but present in the Δ20–22 variant, contains the residues Arg^{672} and Arg^{674}, which are required for sustained generation of IP_3 in response to BCR crosslinking (28). These residues also interact both with phosphorylated Tyr^{348} in Syk when Syk is phosphorylated on both Tyr^{348} and Tyr^{352} (29, 30) and with the activating tyrosine, Tyr^{759}, in the linker region of the γ-SA (31). PLAID patients that have either variant of PLC-γ2 have various immune abnormalities in their B cells. Even though both of the PLAID-associated variant PLC-γ2 proteins, Δ20–22 and Δ19, when expressed in COS-7 cells result in enhanced basal and Rac-activated PLC-γ2 activity, B cells from PLAID patients expressing either variant show defective Ca^{2+} flux and impaired downstream phosphorylation of extracellular signal–regulated kinase (ERK) in response to BCR crosslinking (26). Here, we provide a potential molecular explanation for this apparent paradox by showing that the cSH2 domain of PLC-γ2 is necessary for the assembly of stable signaling complexes that trigger B cell activation in response to BCR crosslinking.

Results

B cells from PLAID patients show transient activation of early BCR signaling components

We evaluated the effect of the PLAID variant PLC-γ2 on early BCR-stimulated signaling events. To do so, we took B cells from healthy donors and PLAID patients carrying a deletion *of PLCG2* exons 20–22 (Δ20–22) and incubated them with $F(ab')_2$ goat antibodies specific for human IgM (anti-IgM) for increasing lengths of time. The cells were then fixed,

permeabilized, and stained with antibodies specific for phosphorylated Igα, Lyn, Syk, Btk, BLNK, and phosphatidylinositol-4,5-bisphosphate 3-kinase (PI3K), as well as with antibodies specific for IgD to identify naïve B cells, and analyzed the cells by flow cytometry. B cells from healthy controls and PLAID patients expressed similar amounts of surface IgM and IgD BCRs. After BCR crosslinking, the extent of phosphorylation of the Iga subunit of BCR was substantially less in B cells from PLAID patients than it was in B cells from healthy donors, but only at the 15-min time point (Fig. 1A), whereas the phosphorylation of Lyn was equivalent in B cells from PLAID patients and healthy donors (Fig. 1B), indicating that these two early B cell signaling events were not markedly compromised by the expression of Δ20–22 variant PLC-γ2. However, as compared to B cells from healthy donors, B cells from PLAID patients showed substantially less phosphorylation of Syk, Btk, and BLNK at most time points (Fig. 1, C to E). Phosphorylation of PI3K was similar in B cells from PLAID patients and healthy donors (Fig. 1F), which excluded the possibility that a failure to activate PI3K contributed to weak BCR-induced Ca^{2+} fluxes in PLAID B cells. Activated PI3K is required for PLC-γ2 activity, because when activated, PI3K phosphorylates PI (4,5) P2 to generate PI (3,4,5) P3, which serves as a docking site on the plasma membrane for PLC-γ2 through its core PH domain (32, 33). Phosphorylation of the mitogen-activated protein kinase (MAPK) ERK (Fig. 2A) was decreased, whereas the phosphorylation of nuclear factor κB (NF-κB) was increased (Fig. 2B) in B cells from PLAID patients compared to B cells from healthy donors; however, phosphorylation of the MAPKs p38 and c-Jun N-terminal kinase (JNK) was not markedly affected (Fig. 2, C and D). Together, these findings suggest that the Δ20–22 variant PLC-γ2 destabilizes the assembly of the early BCR signaling complex, which results in dysregulated signaling downstream of the BCR despite the presence of wild-type PLC-γ2 in B cells from PLAID patients.

BCRs in PLAID B cells expressing the Δ20–22 variant PLC-γ2 fail to properly traffic to intracellular late endosomes or class II–processing compartments

Dependent on appropriate BCR signaling (34), the BCR transports antigen into intracellular compartments in which the antigen is processed and presented on major histocompatibility complex (MHC) class II molecules (35). To assess BCR internalization, we incubated B cells from PLAID patients and healthy donors with biotinylated mouse monoclonal antibody specific for human IgM on ice for 30 min and then washed and warmed the cells to 37°C for increasing lengths of time. The amount of IgM on the surface of mature IgD^+ B cells was then quantified by flow cytometric analysis with Alexa Fluor 647–labeled streptavidin (SA-AF 647). Both the rate of internalization and the amount of BCR internalized were similar in B cells from PLAID patients and those from healthy donors (Fig. 3A).

To monitor the intracellular trafficking of the BCR into transferrin receptor–positive (TfR^+) early endosomes and into late lysosomal-associated membrane protein 1–positive ($LAMP1^+$) endosomes orclass II processing compartments, B cells from a PLAID patient and three healthy donors were incubated with DyLight 549–labeled $F(ab)'_2$ anti-IgM for 30 min on ice and then were warmed to 37°C for increasing lengths of time before being fixed. Cells were permeabilized and stained with DAPI to detect nuclei and with mouse monoclonal antibodies specific for either TfR or LAMP1, which were detected with Alexa

Fluor 647–labeled antibodies specific for mouse IgG, before being imaged by confocal microscopy. We then reconstructed three-dimensional (3D) confocal images from a series of Z section images. Although entry of the BCR into early TfR^+ endosomes at 7 min appeared similar in B cells from the PLAID patient and the healthy donors (Fig. 3, B and C), the BCRs in the B cells from the PLAID patient failed to continue trafficking to $LAMP1^+$ late endosomes orclass II processing compartments. As late as 30 min after warming, the BCRs in the PLAID B cells were still localized in vesicles similar to those observed at 7 min and they showed little co-localization with LAMP1 (Fig. 3, D and E) or with HLA-DM a catalyst for the assembly of peptide MHC class II complexes located in the class II–processing compartments (fig. S1). In contrast, the BCRs in B cells from the healthy donors accumulated in large intracellular compartments that colocalized with LAMP1 (Fig. 3, D and E) and with HLA-DM (fig. S1).

Expression of the Δ20–22 variant PLC-γ2 affects both B cell spreading and BCR clustering in antigen-stimulated B cells

To enable visualization of PLC-γ2, we transiently transfected peripheral blood B cells from healthy donors with plasmids encoding chimeric proteins of green fluorescent protein (GFP) fused to the C-terminus of either wild-type PLC-γ2 or the Δ20–22 variant PLC-γ2, and then we purified GFP-expressing cells by FACS. Cells expressing either wild-type PLC-γ2-GFP or Δ20–22 PLC-γ2-GFP had similar amounts of cell surface BCR (Fig. 4A). In contrast to cells expressing wild-type PLCγ2-GFP, cells expressing Δ20–22 PLCγ2-GFP showed reduced phosphorylation of Syk, BLNK, and Btk when incubated with $F(ab')_2$ anti-IgM antibodies, and failed to flux Ca^{2+} in response to BCR crosslinking on bilayers containing anti-IgM (Fig. 4, B and C). Thus, the transient expression of Δ20–22 PLC-γ2-GFP in peripheral blood B cells from healthy donors recapitulated the defects in BCR signaling observed in B cells from PLAID patients.

B cells expressing Δ20–22 PLC-γ2 were imaged by total internal reflection fluorescence (TIRF) microscopy as they first encountered anti-IgM antibody incorporated into fluid lipid bilayers (anti-IgM bilayers). TIRF microscopy provides a high-resolution image of the plasma membrane, which enabled an assessment of the effect of Δ20–22 PLC-γ2 on the dynamics of BCR clustering and the association of PLC-γ2 and other signaling components with clustered BCRs. As previously described for wild-type human peripheral blood B cells (36), B cells transiently expressing wild-type PLC-γ2-GFP first contacted the anti-IgM bilayer at discrete points, which led to further contact of the B cell with the bilayer, spreading of the cell over the bilayer, and stable accumulation of BCRs in the contact area (Fig. 5, A to C and movie S1). In contrast, B cells expressing Δ20–22 PLC-γ2-GFP showed greater spreading over the bilayer and achieved substantially larger contact areas (Fig. 5, A and B). Because B cell spreading is an actin-dependent process, and PLC-γ2 regulates actin dynamics through several pathways, we attribute this enhanced spreading to a dysregulation of actin polymerization. However, although the BCRs in B cells expressing Δ20–22 PLC-γ2-GFP rapidly accumulated in the contact area during the first 120 s, the accumulation was transient, and these cells had substantially less BCR in the contact area 240 to 300 s after contact than did B cells expressing wild-type PLC-γ2-GFP (Fig. 5C).

The transient accumulation of BCRs in the contact area suggested a possible failure of BCRs in cells expressing Δ20–22 PLC-γ2 to form stable clusters. To quantify BCR clustering, we labeled cells with DyLight 649-Fab anti-IgM to visualize the BCRs, placed the cells on anti-IgM bilayers, and imaged them by TIRF microscopy every 2 s beginning with the initial contact of the cells with the bilayer. To obtain accurate information on the size and fluorescence intensity of each microcluster, the 2D fluorescence intensity profiles of individual BCR clusters at each time point were fitted by a 2D Gaussian function, and 3D surface plots for each image were obtained as previously described (37). To minimize tracking and Gaussian fitting errors, only the first 120 s of each microcluster track was analyzed, although most of the tracks persisted for a maximum of 60 s. We prepared TIRF images and pseudocolor 3D surface plots of representative BCR clusters that were monitored for 120 s (Fig. 5D and movie S2), as well as of the size (Fig. 5E) and average fluorescence intensity (Fig. 5F) of a large number of BCR clusters that were monitored for 60 s. As compared to BCRs on cells expressing Δ20–22 PLC-γ2-GFP, BCRs on cells expressing wild-type PLC-γ2-GFP increased in both fluorescence intensity and size more rapidly, and they eventually formed larger clusters of increased fluorescence intensity.

B cells expressing Δ20–22 PLC-γ2 fail to colocalize signaling components with the BCR after antigen binding to the BCR

To determine whether the failure of BCRs in B cells expressing Δ20–22 PLCγ-GFP to robustly cluster reflected defects in the recruitment or co-localization of Δ20–22 PLC-γ2-GFP with the BCR after receptor crosslinking, we used TIRF microscopy to image both the BCR and PLC-γ2-GFP in B cells placed on anti-IgM bilayers. We observed no differences in the amounts of wild-type PLC-γ2-GFP and Δ20–22 PLC-γ2-GFP at the plasma membrane after BCR stimulation with antigen (Fig. 6A), consistent with the observation that PI3K activation was similar in PLAID B cells and in B cells from healthy donors. However, the extent of colocalization of PLC-γ2 and the BCR was substantially less in B cells expressing Δ20–22 PLC-γ2-GFP incubated on an anti-IgM bilayer than that in cells expressing wild-type PLC-γ2-GFP (Fig 6, B and C and movie S3). After B cells were placed on the anti-IgM bilayers for 15 min, the colocalization of PLC-γ2 and the BCR was substantially lower in B cells expressing Δ20–22 PLC-γ2-GFP than in B cells expressing only wild-type PLC-γ2-GFP (Fig. 6D).

The failure of Δ20–22 PLC-γ2-GFP to colocalize with the BCR suggested that other components of the early BCR signaling complex with which PLC-γ2 directly or indirectly interacts might also fail to colocalize with the BCR. To test this possibility, we labeled B cells transiently expressing either wild-type PLC-γ2-GFP or Δ20–22 PLC-γ2-GFP with DyLight 649-Fab anti-IgM and placed them on anti-IgM bilayers for 5 or 15 min. We then fixed, permeabilized, and stained the cells with antibodies specific for pLyn, pSyk, pBtk, or pPI3K. When comparing B cells expressing wild-type PLC-γ2-GFP with B cells expressing Δ20–22 PLC-γ2-GFP, we found that there were no substantial differences in the amount of pLyn in the contact areas or in the extent of colocalization of pLyn with the BCR (Fig. 7A). However, less pBtk was recruited to the plasma membrane in B cells expressing Δ20–22 PLC-γ2-GFP than was recruited in B cells expressing wild-type PLC-γ2-GFP, whereas substantially less pSyk and pBtk colocalized with the BCR at the 15-min time point in cells

expressing Δ20–22 PLC-γ2-GFP than occurred in cells expressing WT PLCγ2-GFP (Fig. 7, B, and C). There was no difference in the amount of pPI3K in the contact areas of B cells expressing wild-type PLC-γ2-GFP or Δ20–22 PLC-γ2-GFP, nor was there any difference in its colocalization with the BCR (Fig. 7D). Together, these results suggest that stable, signaling-competent BCR clusters containing pSyk, pBLNK, pBtk and PLC-γ2 fail to form in B cells expressing Δ20–22 PLC-γ2-GFP.

B cells expressing Δ19 PLCγ2-GFP fail to flux Ca^{2+} or to exhibit colocalization of PLC-γ2 with the BCR after antigen binding

We next determined whether B cells expressing the Δ19 PLC-γ2 variant, which is devoid of only the N-terminal part of the cSH2 domain, showed similar signaling defects as those observed for B cells expressing the Δ20–22 PLC-γ2 variant, which is devoid of the C-terminal part of the cSH2 domain, the linker region, and the SH3 domain. We transiently transfected peripheral blood B cells from healthy donors with plasmids encoding chimeric proteins of GFP fused to the C terminus of either wild-type PLC-γ2 or the Δ19 PLC-γ2 variant. We first purified cells expressing either wild-type PLC-γ2-GFP or Δ19 PLC-γ2-GFP by FACS and then showed that they expressed similar cell surface amounts of BCR (Fig. 8A). When placed on anti-IgM–containing bilayers, B cells expressing Δ19 PLC-γ2-GFP showed only weak Ca^{2+} flux compared to that of B cells expressing wild-type PLCγ2-GFP (Fig. 8B), similar to what was observed for B cells expressing Δ20–22 PLC-γ2-GFP (Fig. 4C). Although PLC-γ2 was recruited to the plasma membrane equivalently in cells expressing Δ19 PLC-γ2-GFP or wild-type PLC-γ2-GFP (Fig. 8C), there was decreased antigen-dependent colocalization of PLC-γ2 with the BCR in B cells expressing Δ19 PLC-γ2-GFP (Fig. 8D), as was observed for B cells expressing Δ20–22 PLC-γ2-GFP (Fig. 6C). However, B cells expressing Δ19 PLC-γ2-GFP appeared to spread over the anti-IgM–containing bilayers to the same extent as did B cells expressing wild-type PLC-γ2-GFP (Fig. 8E), which was unlike B cells expressing Δ20–22 PLC-γ2-GFP, which showed enhanced spreading (Fig. 5B). This difference suggests the possibility that the SH3 domain present in Δ19 PLC-γ2, but absent from Δ20–22 PLC-γ2, is necessary for the regulation of actin dynamics. B cells expressing Δ19 PLC-γ2-GFP also accumulated substantially fewer BCRs in the contact area over the first 60 s of antigen stimulation than did B cells expressing wild-type PLC-γ2-GFP (Fig. 8F), which is similar to what was observed for B cells expressing Δ20–22 PLC-γ2-GFP.

Together, these results suggest that deletion of the C-terminal part of the cSH2 domain, the linker region, and the SH3 domain of the γ-SA (in the Δ20–22 PLC-γ2 variant) produced a similar phenotype to that caused by deletion of the N-terminal region of the cSH2 domain (in the Δ19 PLC-γ2 variant). Moreover, deletion of either the C- or N-terminal region of the cSH2 domain of PLC-γ2 was sufficient to reduce the ability of B cells to flux Ca^{2+} or to exhibit colocalization of PLC-γ2 with antigen-stimulated BCRs.

Cbl, a suppressor of Ca^{2+} signaling, is aberrantly colocalized with the BCR in B cells expressing Δ20–22 PLC-γ2-GFP

In addition to acting as an adaptor for Syk, Btk, and PLC-γ2, BLNK also associates with the suppressor of B cell signaling, Cbl, which blocks the association of PLC-γ2 with BLNK

(38). Indeed, in human B cells, the Cbl-interacting protein of 85 kD (CIN85) constitutively associates with Cbl and BLNK, and functions to increase the phosphorylation of Cbl, which results in decreased phosphorylation of PLC-γ2 and inhibition of Ca^{2+} flux (39). These observations raised the possibility that the failure of BLNK to form a stable complex with Syk, Btk, and PLC-γ2 directly or indirectly enables the increased association of Cbl with BLNK, further inhibiting PLC-γ2 activity. To investigate this possibility, we imaged the BCR and phosphorylated Cbl (pCbl) in B cells transiently expressing either wild-type PLC-γ2-GFP or Δ20–22 PLC-γ2-GFP 5 and 15 min after the B cells were placed on anti-IgM bilayers. At each time point, the B cells on the bilayer were fixed, permeabilized, and stained with fluorescent anti-IgM or fluorescent antibodies specific for pCbl, and then were imaged by TIRF microscopy. In B cells expressing wild-type PLC-γ2, pCBL was present at the plasma membrane 5 min after BCR crosslinking, and it colocalized with BCRs that were distributed across the entire contact area (Fig. 9). However, at 15 min after BCR crosslinking, when the B cells had further spread, the BCRs were concentrated in the center of the contact area, and pCBL was markedly excluded from this area, which resulted in a decrease in the extent of its colocalization with the BCR. In contrast, in B cells expressing Δ20–22 PLC-γ2-GFP, less pCBL was present in the contact area 5 min after BCR crosslinking, which resulted in decreased colocalization with the BCR. However, after 15 min, the amount of pCBL present in the contact area was similar to that in B cells expressing wild-type PLCγ2-GFP, but pCBL was not excluded from the BCR area, which led to its enhanced colocalization with the BCR. These findings suggest that more pCBL is recruited to the relatively unstable BCR-containing clusters found in B cells expressing Δ20–22 PLC-γ2-GFP, and that it remains colocalized with these clusters.

Discussion

B cells in PLAID patients expressing both a wild-type and a constitutively active variant PLC-γ2 show impaired Ca^{2+} fluxes and ERK signaling in response to BCR crosslinking (26). These signaling deficits were attributed to the loss of the cSH2 domain in PLC-γ2, in part, because PLAID patients expressing either a Δ20–22 variant, which results in loss of part of the cSH2 domain as well as the linker region and the SH3 domain, or a Δ19 variant, which results in the loss of only part of the cSH2 domain, showed indistinguishable PLC-γ2 enzyme activity, as well as impaired Ca^{2+} flux and downstream signaling to ERK in response to BCR crosslinking. Here, we provided a detailed characterization of the effect of the expression of either the Δ20–22 PLC-γ2 variant or the Δ19 PLC-γ2 variant on early events in BCR signaling. The picture that emerged from this analysis is one in which the variant PLC-γ2 acts in a dominant-negative manner to prevent the formation of stable, signaling-competent BCR clusters consisting of pSyk, pBLNK, pBtk, and PLC-γ2. Together with the failure to form stable signaling complexes, the spatial and temporal association with the BCR of the inhibitor of Ca^{2+} signaling, Cbl, was dysregulated in B cells expressing the Δ20–22 PLC-γ2 variant. This apparent requirement for the interactions of multiple components to form stable BCR signaling complexes is similar to that suggested by Weber *et al*. (22) who used TIRF microscopy to demonstrate a requirement for the recruitment of PLC-γ2 to antigen-engaged BCRs through a BLNK- and Btk-dependent mechanism for the formation of microsignalosomes and the coordination of BCR-induced spreading of B cells.

How might the expression of a gain-of-function variant PLC-γ2 result in a loss-of-function phenotype in B cells? One possibility is that the cSH2 domain that is deleted in the Δ20–22 variant PLC-γ2 acts not only to autoinhibit the catalytic domain of PLC-γ2, but once phosphorylated and released from its interaction with the catalytic domain, it also functions as an interaction domain that stabilizes the PLC-γ2:pSyk:pBLNK:pBtk complex. Support for this possibility comes from the characterization of a gain-of-function point mutation (S707Y) in the cSH2 domain of PLC-γ2 in what are termed autoinflammation and PLAID (APLAID) patients (27). Crosslinking of the BCR on B cells from APLAID patients results in substantially increased phosphorylation of ERK as compared to that in B cells from either healthy donors or PLAID patients. In this case, the expression of a constitutively active mutant PLC-γ2 resulted in enhanced PLC-γ2 signaling, which is in contrast to the decreased PLC-γ2 signaling that resulted from the expression of a constitutively active PLC-γ2 variant devoid of the cSH2. This suggests that the cSH2 domain serves a function in immune cell signaling in addition to its role in masking the active site of PLC-γ2. Indeed, the cSH2 domain of PLC-γ2 interacts with Syk when both Tyr^{342} and Tyr^{346} of Syk are phosphorylated (29). In addition, the cSH2 domain of PLC-γ1 docks with Btk through an acidic patch centered on the G helix of Btk, and mutations of these critical residues in Btk impairs the efficacy of the phosphorylation of PLC-γ1 by Btk, not by altering its catalytic activity, but by altering its ability to recognize PLC-γ1 as a substrate (40). One could imagine that interactions between the cSH2 domain of PLC-γ2 and Syk and Btk act to stabilize the complex consisting of the BCR, pSyk, pBLNK, pPLC-γ2, and pBtk. We observed that Cbl, an inhibitor of PLC-γ2 (39), was aberrantly colocalized with the BCR in B cells expressing Δ20–22 PLC-γ2, but not in B cells expressing wild-type PLC-γ2. The altered association of Cbl with the BCR could affect PLC-γ2 activity by targeting Syk for ubiquitination and degradation, a function we previously described for Cbl (41). A second, nonexclusive, possibility is that constitutively active PLC-γ2 establishes a strong inhibitory response that reduces the enzymatic activity of PLC-γ2 by some unknown mechanism.

The data presented here paint a highly dynamic picture of the BCR signalosome in which multiple interactions between the domains of the signaling components serve to stabilize the complex and enhance signaling. Cruz-Orcutt *et al*. (42) presented a model for the activation of PLC-γ1 in T cells in which PLC-γ1 and the adaptor protein LAT transiently interact to catalyze the activation of PLC-γ1, which then translocates to the T cell receptor (TCR) complex or to other structures. Such dynamic spatial organization of PLC-γ2 is certainly possible in B cells. Indeed, we observed equivalent recruitment of Δ20–22 PLC-γ2, Δ19 PLC-γ2, and wild-type PLC-γ2 to the plasma membrane of B cells after BCR engagement, but we found less colocalization of Δ20–22 PLC-γ2 and Δ19 PLC-γ2 with the BCR as compared to wild-type PLC-γ2, which suggests an initial association of PLC-γ2 with unstimulated BCR structures; however, what these structures might be is not yet known.

In addition to demonstrating the failure of B cells expressing Δ20–22 PLC-γ2 to form stable BCR signaling complexes, we also provided evidence that the BCRs, although internalized normally into TfR^{+} early endosomes after BCR crosslinking, failed to properly traffic to the $LAMP1^{+}$ late endosome/class II processing compartments. Various studies have established that the internalization and proper trafficking of the BCR into antigen-processing

compartments requires BCR signaling (34), and the failure of PLAID B cells to form a stable signaling complex could clearly influence trafficking. In addition, Schnyder *et al*. (43) demonstrated that Cbl, together with Grb2 and Dok-3, is recruited to BCR microclusters, and that although Cbl is dispensable for the formation of microclusters and B cell spreading, Cbl is necessary for B cell contraction and the process of concentration of BCR-bound antigen on the B cell surface through its association with the microtubule motor protein dynein. It is an interesting possibility that the aberrant colocalization of Cbl with BCR clusters in B cells expressing Δ20–22 PLC-γ2 might eventually affect proper antigen-gathering and trafficking of the BCR and antigen. The inability to properly traffic BCR-bound antigen could contribute to the PLAID syndrome by decreasing antigen-specific interactions between B and T cells, which are necessary for the activation of B cells and their differentiation into antibody-secreting cells and the generation of memory B cells.

Materials and Methods

Study subjects

Subjects were admitted to the National Institutes of Health Clinical Center, where they were enrolled in clinical protocols approved by the institutional review board of the National Institute of Allergy and Infectious Diseases, as previously described (26).

Cells, plasmids, and transient transfections

B cells were isolated from PBMCs by negative selection with a MACS human B cell isolation kit II (Miltenyi Biotec). B cells were transiently transfected with plasmids encoding wild-type (WT) PLC-γ2-GFP, Δ20–22 PLC-γ2-GFP, or Δ19 PLC-γ2-GFP, which were constructed as previously described (26), with an Amaxa human B cell Nucleofection Kit (Lonza) and program U-015. Transfected B cells were cultured overnight, and GFP^+ cells were obtained by FACS.

Flow cytometric analysis

The cell surface expression of the BCR in B cells expressing WT PLC-γ2-GFP, Δ20–22 PLC-γ2-GFP, or Δ19 PLC-γ2-GFP was quantified by labeling the cells on ice with Alexa Fluor 647–conjugated goat Fab anti-human IgM. Propidium iodide (PI) was added to distinguish between live and dead cells. The PI^-, GFP^+, and IgM^+ cells were gated to analyze cell surface BCR expression. To detect intracellular phosphorylated proteins, cells were incubated with $F(ab')_2$ anti-IgM (10 μg/ml), fixed with 4% paraformaldehyde (PFA), permeabilized with 90% methanol, and stained with rabbit antibodies specific for pCD79A (Iga, Tyr^{182}) (pIgα), pSyk (Tyr^{352}), pPI3K p85 (Tyr^{458})/p55 (Tyr^{199}) (all of which were obtained from Cell Signaling); pLyn (Tyr^{396}, Abcam); pNF-κB p65 (Ser^{536}, Santa Cruz); pJNK (Thr^{183}/Tyr^{185}, BD Pharmingen); or pp38 MAPK (Thr^{180}/Tyr^{182}, R&D Systems). Rabbit antibodies were detected with phycoerythrin (PE)- or Alexa Fluor 647–conjugated goat antibodies specific for rabbit IgG (Jackson ImmunoResearch Laboratories). PE-conjugated rabbit monoclonal antibody specific for pp44/p42 MAPK (ERK1/2, Thr^{202}/Thr^{204}, Cell Signaling) and PE-conjugated mouse monoclonal antibody specific for pBtk (Tyr^{223}) or pBLNK (Tyr^{84}) (both from *BD* Biosciences) were also used. The internalization of cell-surface BCR was quantified as described previously (44). Briefly, B cells were

incubated with biotinylated mouse monoclonal antibody specific for human IgM (10 μg/ml) on ice for 30 min, washed, and incubated at 37°C. Cells were stained on ice with Alexa Fluor 647–conjugated streptavidin (SA-AF 647) and fluorescein isothiocyanate (FITC)-conjugated $F(ab)'_2$ anti-IgD to gate on naïve B cells, and the amount of cell surface BCR was quantified by flow cytometry.

Confocal microscopy and 3D colocalization analysis

To analyze the intracellular trafficking of the BCR, confocal microscopy was performed as previously described (45). Briefly, PBMCs from either a healthy donor or a PLAID patient were placed on poly-D-Lysine–coated chamber slides (BD Biosciences) and incubated with DyLight 549–labeled $F(ab')_2$ anti-IgM (20 μg/ml) on ice, washed, and chased at 37°C for the indicated times. Cells were fixed with 4% PFA, permeabilized with 0.1% Triton X-100, and labeled with mouse monoclonal antibodies specific for CD107a/(LAMP1) (BD Biosciences), CD71/TfR (BD Biosciences), or HLA-DM (Santa Cruz), which were then detected with either Alexa Fluor 647– or Alexa Fluor 488–conjugated goat antibodies specific for mouse IgG. DAPI was used for nuclear staining. A Zeiss 710 laser scanning microscope (LSM) equipped with a 63×, 1.45 NA oil objective lens was used for three-color Z stack images with three laser lines (UV, 568 nm, and 633 nm) under the setting of image acquisition without crosstalk between two colors, and 0.46-μm optimal Z sections controlled by ZEN software (Carl ZEISS). The reconstruction of 3D surface images for BCR, either TfR or LAMP1, colocalized voxels, and merged images, and the analysis of 3D Pearson's colocalization coefficient (R) were obtained with Imaris software (Bitplane) using the surface reconstruction tool and the 3D colocalization analysis tool, respectively, with an automatic background threshold–setting algorithm provided by Imaris at the above background level for each 3D image. The colocalization coefficient of the BCR and HLA-DM (the ratio of the number of pixels that contain both HLA DM and BCR to the total number of pixels that contain BCR) was calculated from 2D images using the colocalization analysis program in ZEN software 2010 (Carl ZEISS) after setting the threshold on the background region of interest.

Ca^{2+} flux assay in cells on a planar lipid bilayer

Human peripheral blood B cells were transiently transfected with plasmids encoding WT PLC-γ2-GFP, Δ20–22 PLC-γ2-GFP, or Δ19 PLC-γ2-GFP and then were sorted to isolate the GFP^+ naïve B cells. Cells were labeled with the calcium indicator dye Fluo-4 (Invitrogen), placed on anti-IgM bilayers pre-warmed to 37°C, and live-cell images were acquired at 2-s intervals by epifluorescence microscopy. Images were quantified by calculating the ratio of the mean fluorescence intensity (MFI) of Fluo-4 at each time point to the MFI of the first frame in which the cell appeared in the image field, after subtracting the MFI of the background region of interest.

Total internal reflection fluorescence (TIRF) microscopy

Planar lipid bilayers containing biotinylated $F(ab')_2$ anti-IgM bound to streptavidin-lipids (anti-IgM bilayers) were prepared as described previously (46). Time-lapse, live-cell TIRF imaging was performed with an Olympus IX-81 TIRF microscope system, as detailed previously (36, 37, 47). For fixed-cell imaging, cells were placed on anti-IgM bilayers at

37°C for the times indicated in the figure legends and then were fixed in 4% PFA, permeabilized, and stained with rabbit anti-pLyn (Tyr^{396}, Abcam), anti-pBtk (Tyr^{551}, Abcam), anti-pSyk (Cell Signaling), anti-pPI3K (Cell Signaling), or anti-pCbl (Santa Cruz), followed by Alexa Fluor 568–conjugated $F(ab')_2$ goat antibodies specific for rabbit IgG (H +L). To analyze the contact area of B cells with the anti-IgM bilayers, the MFI values of BCR, pLyn, pSyk, pBtk, pPI3K, and pCbl within the contact area (per unit area) were analyzed by Image Pro Plus (Media Cybernetics), ImageJ (NIH), or Matlab (Mathworks) software. The Pearson's colocalization coefficients (R) between any two molecules were obtained from background-subtracted images by intensity correlation analysis with the Wright Cell Imaging Facility plugin of ImageJ, as described previously (36, 48, 49).

Analysis of the fluorescence intensities and sizes of BCR microclusters

Tracking of single BCR microclusters and 2D Gaussian analyses were performed as described previously (37, 47). Briefly, each BCR microcluster in time-lapse TIRF images was processed by means of least-square fitting of a 2D Gaussian function at each time point (50). For each microcluster, the fit yields the integrated fluorescence intensity (FI) and generalized full width at half-maximum peak height (FWHM) of the intensity distribution in the x and y direction. Only microclusters that were successfully tracked for at least 10 steps and only the first 30 steps (60 s) of each microcluster track in transfected primary B cells were selected for analysis to avoid tracking and Gaussian fitting errors that arise from spots merging and overlapping at later stages of the observed processes. Values belonging to the same track were normalized to the first position.

Statistical analyses

Statistically significant differences between datasets were determined with either the unpaired Student's *t* test (when comparing two variables) or ANOVA (for more than two variables) with Prism 6 software (GraphPad). All P values were two-sided, and $P < 0.05$ was considered to be statistically significant.

Supplementary Material

Refer to Web version on PubMed Central for supplementary material.

Acknowledgments

We thank J. Brzostowski for expert advice on imaging. **Funding:** This work was supported by the Intramural Research Program of the National Institute of Allergy and Infectious Diseases, National Institutes of Health.

References

1. Kurosaki T, Hikida M. Tyrosine kinases and their substrates in B lymphocytes. Immunol Rev. 2009; 228:132–148. [PubMed: 19290925]
2. Kadamur G, Ross EM. Mammalian phospholipase C. Annual review of physiology. 2013; 75:127–154.
3. Scharenberg AM, Humphries LA, Rawlings DJ. Calcium signalling and cell-fate choice in B cells. Nat Rev Immunol. 2007; 7:778–789. [PubMed: 17853903]
4. Hilgemann DW. Local PIP(2) signals: when, where, and how? Pflugers Archiv: European journal of physiology. 2007; 455:55–67. [PubMed: 17534652]

5. Saito K, Tolias KF, Saci A, Koon HB, Humphries LA, Scharenberg A, Rawlings DJ, Kinet JP, Carpenter CL. BTK regulates PtdIns-4,5-P2 synthesis: importance for calcium signaling and PI3K activity. Immunity. 2003; 19:669–678. [PubMed: 14614854]
6. Baba Y, Kurosaki T. Impact of Ca2+ signaling on B cell function. Trends Immunol. 2011; 32:589–594. [PubMed: 22000665]
7. Bunney TD, Katan M. PLC regulation: emerging pictures for molecular mechanisms. Trends in biochemical sciences. 2011; 36:88–96. [PubMed: 20870410]
8. Everett KL, Buehler A, Bunney TD, Margineanu A, Baxendale RW, Vatter P, Retlich M, Walliser C, Manning HB, Neil MA, Dunsby C, French PM, Gierschik P, Katan M. Membrane environment exerts an important influence on racmediated activation of phospholipase Cgamma2. Mol Cell Biol. 2011; 31:1240–1251. [PubMed: 21245382]
9. Gresset A, Hicks SN, Harden TK, Sondek J. Mechanism of phosphorylation-induced activation of phospholipase C-gamma isozymes. J Biol Chem. 2010; 285:35836–35847. [PubMed: 20807769]
10. Bunney TD, Esposito D, Mas-Droux C, Lamber E, Baxendale RW, Martins M, Cole A, Svergun D, Driscoll PC, Katan M. Structural and functional integration of the PLCgamma interaction domains critical for regulatory mechanisms and signaling deregulation. Structure. 2012; 20:2062–2075. [PubMed: 23063561]
11. Saouaf SJ, Mahajan S, Rowley RB, Kut SA, Fargnoli J, Burkhardt AL, Tsukada S, Witte ON, Bolen JB. Temporal differences in the activation of three classes of non-transmembrane protein tyrosine kinases following B-cell antigen receptor surface engagement. Proceedings of the National Academy of Sciences of the United States of America. 1994; 91:9524–9528. [PubMed: 7524079]
12. Rolli V, Gallwitz M, Wossning T, Flemming A, Schamel WW, Zurn C, Reth M. Amplification of B cell antigen receptor signaling by a Syk/ITAM positive feedback loop. Mol Cell. 2002; 10:1057–1069. [PubMed: 12453414]
13. Oellerich T, Bremes V, Neumann K, Bohnenberger H, Dittmann K, Hsiao HH, Engelke M, Schnyder T, Batista FD, Urlaub H, Wienands J. The B-cell antigen receptor signals through a preformed transducer module of SLP65 and CIN85. EMBO J. 2011; 30:3620–3634. [PubMed: 21822214]
14. Fu C, Turck CW, Kurosaki T, Chan AC. BLNK: a central linker protein in B cell activation. Immunity. 1998; 9:93–103. [PubMed: 9697839]
15. Kulathu Y, Hobeika E, Turchinovich G, Reth M. The kinase Syk as an adaptor controlling sustained calcium signalling and B-cell development. EMBO J. 2008; 27:1333–1344. [PubMed: 18369315]
16. Rawlings DJ, Saffran DC, Tsukada S, Largaespada DA, Grimaldi JC, Cohen L, Mohr RN, Bazan JF, Howard M, Copeland et a. Mutation of unique region of Bruton's tyrosine kinase in immunodeficient XID mice. Science. 1993; 261:358. [PubMed: 8332901]
17. Li Z, Wahl MI, Eguinoa A, Stephens LR, Hawkins PT, Witte ON. Phosphatidylinositol 3-kinase-gamma activates Bruton's tyrosine kinase in concert with Src family kinases. Proc Natl Acad Sci U S A. 1997; 94:13820–13825. [PubMed: 9391111]
18. Park H, Wahl MI, Afar DE, Turck CW, Rawlings DJ, Tam C, Scharenberg AM, Kinet JP, Witte ON. Regulation of Btk function by a major autophosphorylation site within the SH3 domain. Immunity. 1996; 4:515–525. [PubMed: 8630736]
19. Baba Y, Hashimoto S, Matsushita M, Watanabe D, Kishimoto T, Kurosaki T, Tsukada S. BLNK mediates Syk-dependent Btk activation. Proc Natl Acad Sci U S A. 2001; 98:2582–2586. [PubMed: 11226282]
20. Ishiai M, Kurosaki M, Pappu R, Okawa K, Ronko I, Fu C, Shibata M, Iwamatsu A, Chan AC, Kurosaki T. BLNK required for coupling Syk to PLC gamma 2 and Rac1-JNK in B cells. Immunity. 1999; 10:117–125. [PubMed: 10023776]
21. Engelke M, Oellerich T, Dittmann K, Hsiao HH, Urlaub H, Serve H, Griesinger C, Wienands J. Cutting edge: feed-forward activation of phospholipase Cgamma2 via C2 domain-mediated binding to SLP65. J Immunol. 2013; 191:5354–5358. [PubMed: 24166973]
22. Weber M, Treanor B, Depoil D, Shinohara H, Harwood NE, Hikida M, Kurosaki T, Batista FD. Phospholipase C-gamma2 and Vav cooperate within signaling microclusters to propagate B cell

spreading in response to membrane-bound antigen. J Exp Med. 2008; 205:853–868. [PubMed: 18362175]

23. Fleire SJ, Goldman JP, Carrasco YR, Weber M, Bray D, Batista FD. B cell ligand discrimination through a spreading and contraction response. Science. 2006; 312:738–741. [PubMed: 16675699]
24. DeBell K, Graham L, Reischl I, Serrano C, Bonvini E, Rellahan B. Intramolecular regulation of phospholipase C-gamma1 by its C-terminal Src homology 2 domain. Mol Cell Biol. 2007; 27:854–863. [PubMed: 17116690]
25. Everett KL, Bunney TD, Yoon Y, Rodrigues-Lima F, Harris R, Driscoll PC, Abe K, Fuchs H, de Angelis MH, Yu P, Cho W, Katan M. Characterization of phospholipase C gamma enzymes with gain-of-function mutations. J Biol Chem. 2009; 284:23083–23093. [PubMed: 19531496]
26. Ombrello MJ, Remmers EF, Sun G, Freeman AF, Datta S, Torabi-Parizi P, Subramanian N, Bunney TD, Baxendale RW, Martins MS, Romberg N, Komarow H, Aksentijevich I, Kim HS, Ho J, Cruse G, Jung MY, Gilfillan AM, Metcalfe DD, Nelson C, O'Brien M, Wisch L, Stone K, Douek DC, Gandhi C, Wanderer AA, Lee H, Nelson SF, Shianna KV, Cirulli ET, Goldstein DB, Long EO, Moir S, Meffre E, Holland SM, Kastner DL, Katan M, Hoffman HM, Milner JD. Cold urticaria, immunodeficiency, and autoimmunity related to PLCG2 deletions. N Engl J Med. 2012; 366:330–338. [PubMed: 22236196]
27. Zhou Q, Lee GS, Brady J, Datta S, Katan M, Sheikh A, Martins MS, Bunney TD, Santich BH, Moir S, Kuhns DB, Long Priel DA, Ombrello A, Stone D, Ombrello MJ, Khan J, Milner JD, Kastner DL, Aksentijevich I. A hypermorphic missense mutation in PLCG2, encoding phospholipase Cgamma2, causes a dominantly inherited autoinflammatory disease with immunodeficiency. Am J Hum Genet. 2012; 91:713–720. [PubMed: 23000145]
28. Ishiai M, Sugawara H, Kurosaki M, Kurosaki T. Cutting edge: association of phospholipase C-gamma 2 Src homology 2 domains with BLNK is critical for B cell antigen receptor signaling. J Immunol. 1999; 163:1746–1749. [PubMed: 10438904]
29. Geahlen RL. Syk and pTyr'd: Signaling through the B cell antigen receptor. Biochim Biophys Acta. 2009; 1793:1115–1127. [PubMed: 19306898]
30. Groesch TD, Zhou F, Mattila S, Geahlen RL, Post CB. Structural basis for the requirement of two phosphotyrosine residues in signaling mediated by Syk tyrosine kinase. Journal of molecular biology. 2006; 356:1222–1236. [PubMed: 16410013]
31. Hajicek N, Charpentier TH, Rush JR, Harden TK, Sondek J. Autoinhibition and phosphorylation-induced activation of phospholipase C-gamma isozymes. Biochemistry. 2013; 52:4810–4819. [PubMed: 23777354]
32. Hiller G, Sundler R. Regulation of phospholipase C-gamma 2 via phosphatidylinositol 3-kinase in macrophages. Cellular signalling. 2002; 14:169–173. [PubMed: 11781142]
33. Wang D, Feng J, Wen R, Marine JC, Sangster MY, Parganas E, Hoffmeyer A, Jackson CW, Cleveland JL, Murray PJ, Ihle JN. Phospholipase Cgamma2 is essential in the functions of B cell and several Fc receptors. Immunity. 2000; 13:25–35. [PubMed: 10933392]
34. Siemasko K, Clark MR. The control and facilitation of MHC class II antigen processing by the BCR. Curr Opin Immunol. 2001; 13:32–36. [PubMed: 11154914]
35. Lanzavecchia A. Receptor-mediated antigen uptake and its effect on antigen presentation to class II-restricted T lymphocytes. Annual Review of Immunology. 1990; 8:773–793.
36. Davey AM, Pierce SK. Intrinsic differences in the initiation of B cell receptor signaling favor responses of human IgG(+) memory B cells over IgM(+) naive B cells. J Immunol. 2012; 188:3332–3341. [PubMed: 22379037]
37. Liu W, Meckel T, Tolar P, Sohn HW, Pierce SK. Antigen affinity discrimination is an intrinsic function of the B cell receptor. J Exp Med. 2010; 207:1095–1111. [PubMed: 20404102]
38. Yasuda T, Maeda A, Kurosaki M, Tezuka T, Hironaka K, Yamamoto T, Kurosaki T. Cbl suppresses B cell receptor-mediated phospholipase C (PLC)-gamma2 activation by regulating B cell linker protein-PLC-gamma2 binding. J Exp Med. 2000; 191:641–650. [PubMed: 10684856]
39. Niiro H, Jabbarzadeh-Tabrizi S, Kikushige Y, Shima T, Noda K, Ota S, Tsuzuki H, Inoue Y, Arinobu Y, Iwasaki H, Shimoda S, Baba E, Tsukamoto H, Horiuchi T, Taniyama T, Akashi K. CIN85 is required for Cbl-mediated regulation of antigen receptor signaling in human B cells. Blood. 2012; 119:2263–2273. [PubMed: 22262777]

40. Xie Q, Joseph RE, Fulton DB, Andreotti AH. Substrate recognition of PLCgamma1 via a specific docking surface on Itk. J Mol Biol. 2013; 425:683–696. [PubMed: 23219468]
41. Sohn HW, Gu H, Pierce SK. Cbl-b negatively regulates B cell antigen receptor signaling in mature B cells through ubiquitination of the tyrosine kinase Syk. J Exp Med. 2003; 197:1511–1524. [PubMed: 12771181]
42. Cruz-Orcutt N, Vacaflores A, Connolly SF, Bunnell SC, Houtman JC. Activated PLC-gamma1 is catalytically induced at LAT but activated PLC-gamma1 is localized at both LAT- and TCR-containing complexes. Cellular signalling. 2014; 26:797–805. [PubMed: 24412752]
43. Schnyder T, Castello A, Feest C, Harwood NE, Oellerich T, Urlaub H, Engelke M, Wienands J, Bruckbauer A, Batista FD. B cell receptor-mediated antigen gathering requires ubiquitin ligase Cbl and adaptors Grb2 and Dok-3 to recruit dynein to the signaling microcluster. Immunity. 2011; 34:905–918. [PubMed: 21703542]
44. Stoddart A, Dykstra ML, Brown BK, Song W, Pierce SK, Brodsky FM. Lipid rafts unite signaling cascades with clathrin to regulate BCR internalization. Immunity. 2002; 17:451. [PubMed: 12387739]
45. Sohn HW, Gu H, Pierce SK. Cbl-b negatively regulates BCR signaling in mature B cells through ubiquitination of the tyrosine kinase Syk. J Exp Med. 2003; 197:1511–1524. [PubMed: 12771181]
46. Sohn HW, Tolar P, Brzostowski J, Pierce SK. A method for analyzing protein-protein interactions in the plasma membrane of live B cells by fluorescence resonance energy transfer imaging as acquired by total internal reflection fluorescence microscopy. Methods Mol Biol. 2010; 591:159–183. [PubMed: 19957130]
47. Liu W, Meckel T, Tolar P, Sohn HW, Pierce SK. Intrinsic properties of immunoglobulin IgG1 isotype-switched B cell receptors promote microclustering and the initiation of signaling. Immunity. 2010; 32:778–789. [PubMed: 20620943]
48. Li Q, Lau A, Morris TJ, Guo L, Fordyce CB, Stanley EF. A syntaxin 1, G alpha (o), and N-type calcium channel complex at a presynaptic nerve terminal: analysis by quantitative immunocolocalization. J. Neurosci. 2004; 24:4070–4081. [PubMed: 15102922]
49. Liu W, Won Sohn H, Tolar P, Meckel T, Pierce SK. Antigen-induced oligomerization of the B cell receptor is an early target of FcgRIIB inhibition. J. Immunol. 2010; 184:1977–1989. [PubMed: 20083655]
50. Holtzer L, Meckel T, Schmidt T. Nanometric three-dimensional tracking of individual quantum dots in cells. Applied Physics Letters. 2007; 90

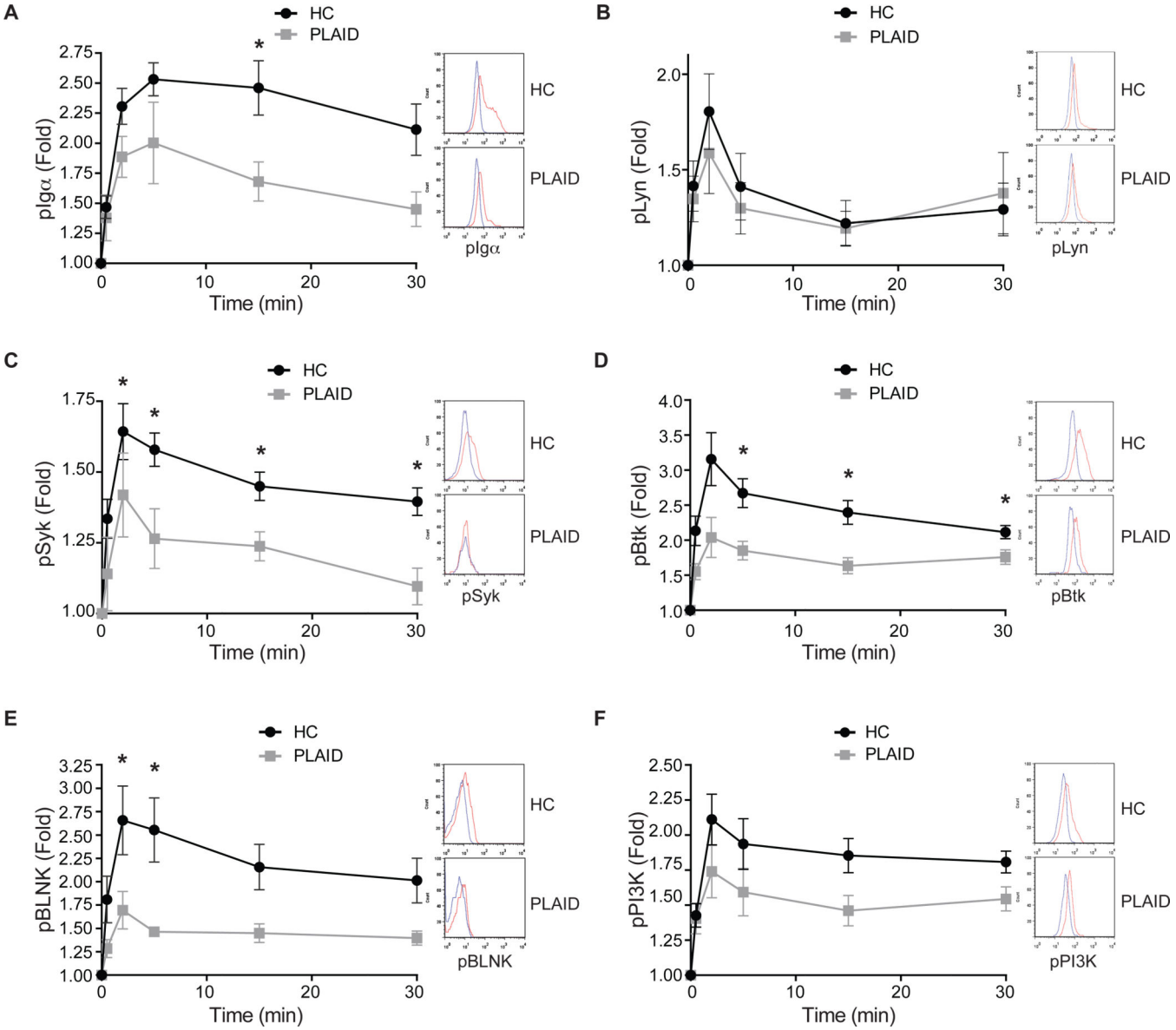

Fig. 1. Altered early BCR signaling after BCR crosslinking in PLAID B cells

(**A** to **F**) PBMCs from either healthy control (HC) donors (n = 8 for pSyk; n = 12 for pPI3K; n = 9 for pBtk, pIgα, and pBLNK; and n = 5 for pLyn) or PLAID patients (n = 4 for pSyk; n = 5 for pPI3K; n = 4 for pBtk, pIgα, and pBLNK; and n = 3 for pLyn) were stimulated with $F(ab')_2$ goat antibodies specific for human IgM (anti-IgM, 10 μg/ml) at 37°C. At the indicated times, cells were fixed on ice, permeabilized, and incubated with antibodies specific for (A) pIgα (Tyr^{182}), (B) pLyn (Tyr^{396}), (C) pSyk (Tyr^{352}), (D) pBtk (Tyr^{223}), (E) pBLNK (Tyr^{84}), or (F) pPI3K p85 (Tyr^{458}), as well as with FITC-labeled $F(ab')_2$ goat antibodies specific for human IgD to enable gating on naïve B cells. Three-color flow cytometric analyses were performed. Graphs shown means ± SEM for fold-increases in the MFI for each phosphorylated protein at the indicated times relative to that of cells at time 0. **P* < 0.05 by student's *t* test. Representative flow cytometry plots for unstimulated cells

(blue line) and for cells stimulated for 5 min with anti-IgM (red line) are shown to the right of each graph.

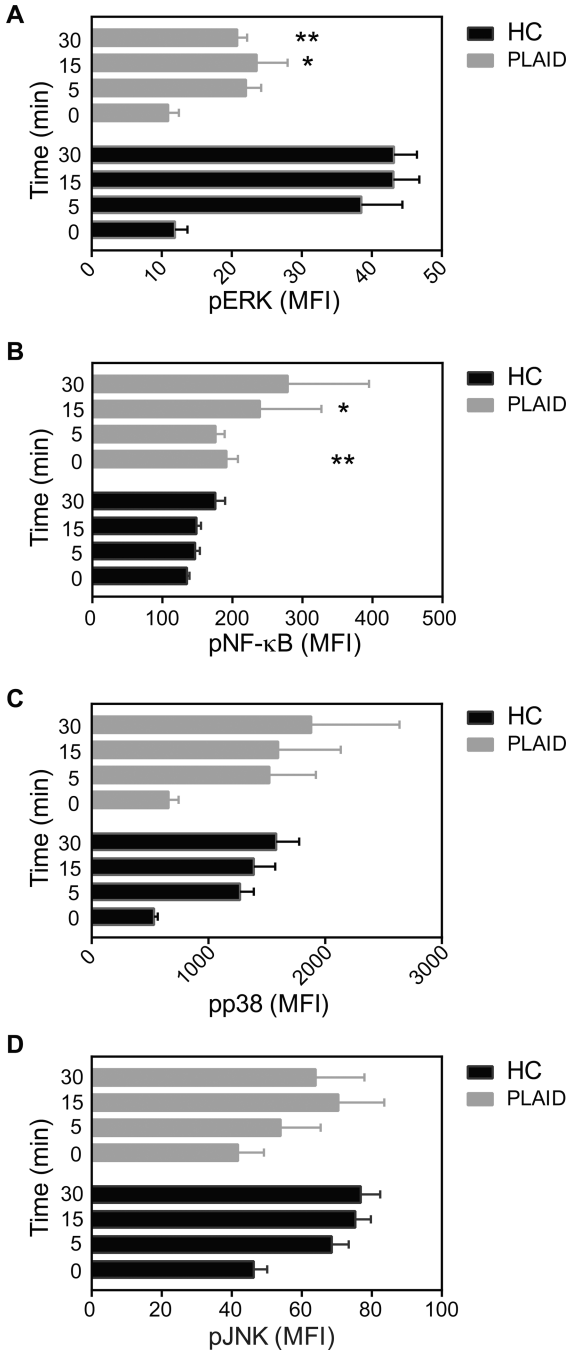

Fig. 2. Altered intermediate kinase signaling upon BCR crosslinking in PLAID B cells

(**A** to **D**) PBMCs from HC donors (n = 3 for pERK; n = 8 for pJNK and pNF-KB; and n = 9 for pp38) or PLAID patients (n = 3 for pERK; n = 2 for pJNK and pNF-KB; and n = 3 for pp38) were analyzed by flow cytometry as described in Fig. 1 for the phosphorylation of (A) ERK, (B) NF-KB, (C) p38 and (D) JNK. Cells were treated with $F(ab')_2$ anti-IgM (10 μg/μl) at 37°C for the indicated times, fixed, permeabilized on ice, and incubated with the appropriate phospho-specific antibodies, as well as with FITC-$F(ab')_2$ anti-IgD to enable gating on naïve B cells. The MFIs of the phosphorylated proteins at the indicated times for IgD^+ naïve B

cells were obtained. Data are means ± SEM of the MFI. *$P < 0.05$, **$P < 0.01$, as determined by the student's *t* test.

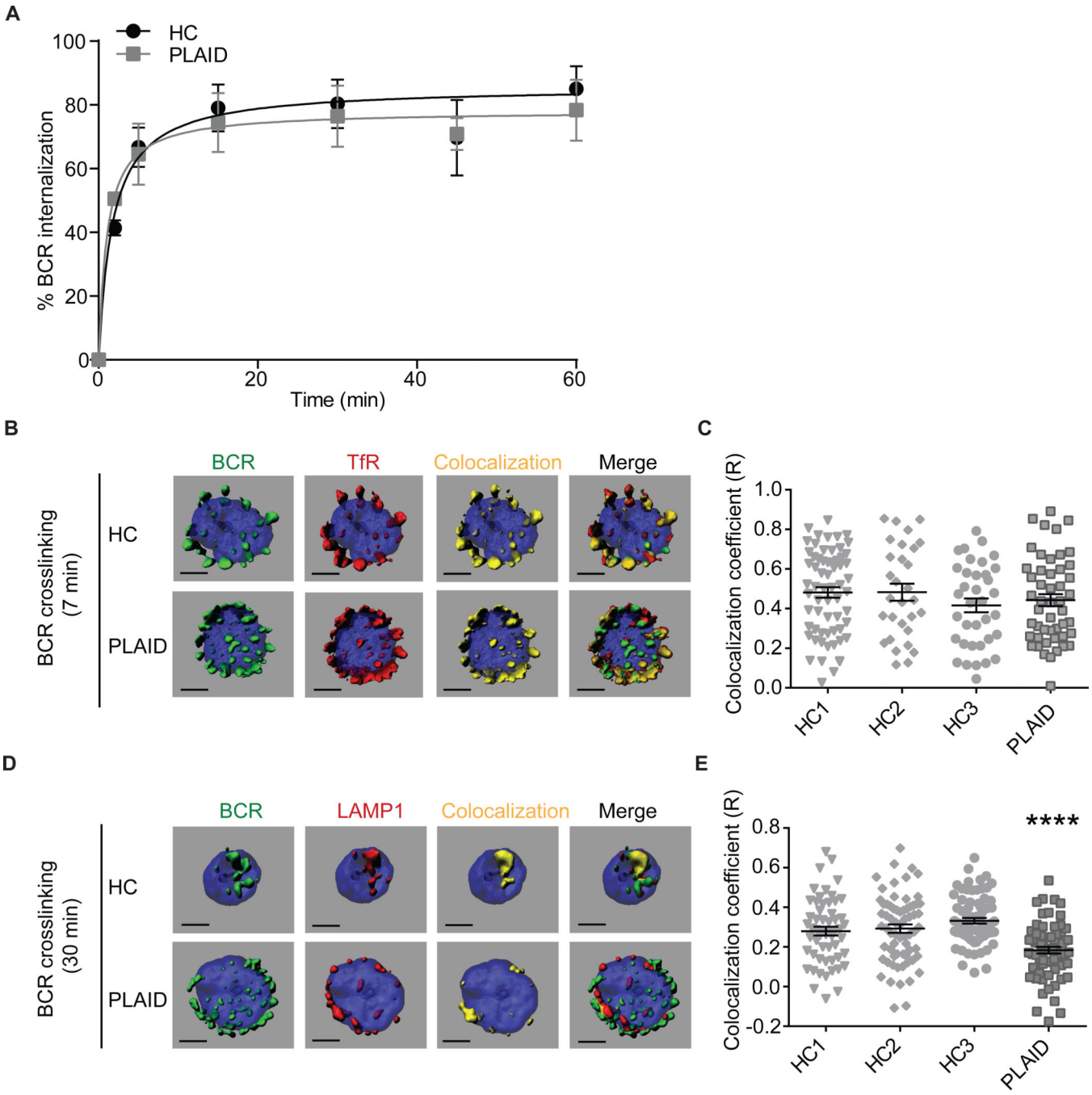

Fig. 3. The effect of the PLAID Δ20–22 variant PLC-γ2 on the internalization and intracellular trafficking of the BCR

(**A**) B cells from PLAID patients (n = 3) and HC donors (n = 6) were incubated with biotinylated mouse monoclonal antibody specific for human IgM (10 μg/ml) on ice for 30 min, washed to remove unbound antibody, and incubated at 37°C for the indicated times. Cells were put on ice and incubated with Alexa Fluor 647–labeled streptavidin to quantify the cell surface abundance of the BCR, as well as with FITC-F(ab)'$_2$ anti-IgD to identify naïve B cells. Data are means ± SEM of the percentage of the BCR that was internalized. (**B** to **E**) B cells from three HC donors and one PLAID patient were incubated with Alexa Fluor

549–labeled F(ab)'$_2$ anti-IgM on ice for 30 min to crosslink the BCR, washed, and warmed to 37°C for the indicated times. Cells were permeabilized, stained with the nuclear stain DAPI, as well as with mouse monoclonal antibodies specific for either TfR or LAMP1, which were detected with Alexa Fluor 647–labeled antibodies against mouse IgG. Cells were then fixed and imaged by confocal microscopy. Shown are the reconstituted 3D surface images from a single HC donor and the PLAID patient of BCR (green), TfR (red), colocalization voxels (yellow), and merged images of the three targets with DAPI (blue) from Z stack confocal images taken at (B) 7 min and (D) 30 min after warming to 37°C. Pearson's colocalization coefficients (R) were calculated for all three HCs and the PLAID patient for the 3D images at (C) 7 min and (E) 30 min after warming to 37°C. The 3D surface images were reconstituted and the Pearson's colocalization coefficient (R) per cell was calculated. Graphs show means ± SEM for B cells from HC1 (n = 64 cells), HC2 (n = 30 cells), HC3 (n = 36 cells), and the PLAID patient (n = 49 cells) for the time point represented in (B), as well as from HC1 (n = 56 cells), HC2 (n =67 cells), HC3 (n =74 cells), and the PLAID patient (n = 69 cells) for the time point represented in (D), and are from one of two repeated experiments. ****$P < 0.001$ by unpaired student's *t* test. Scale bar: 2.5 μm.

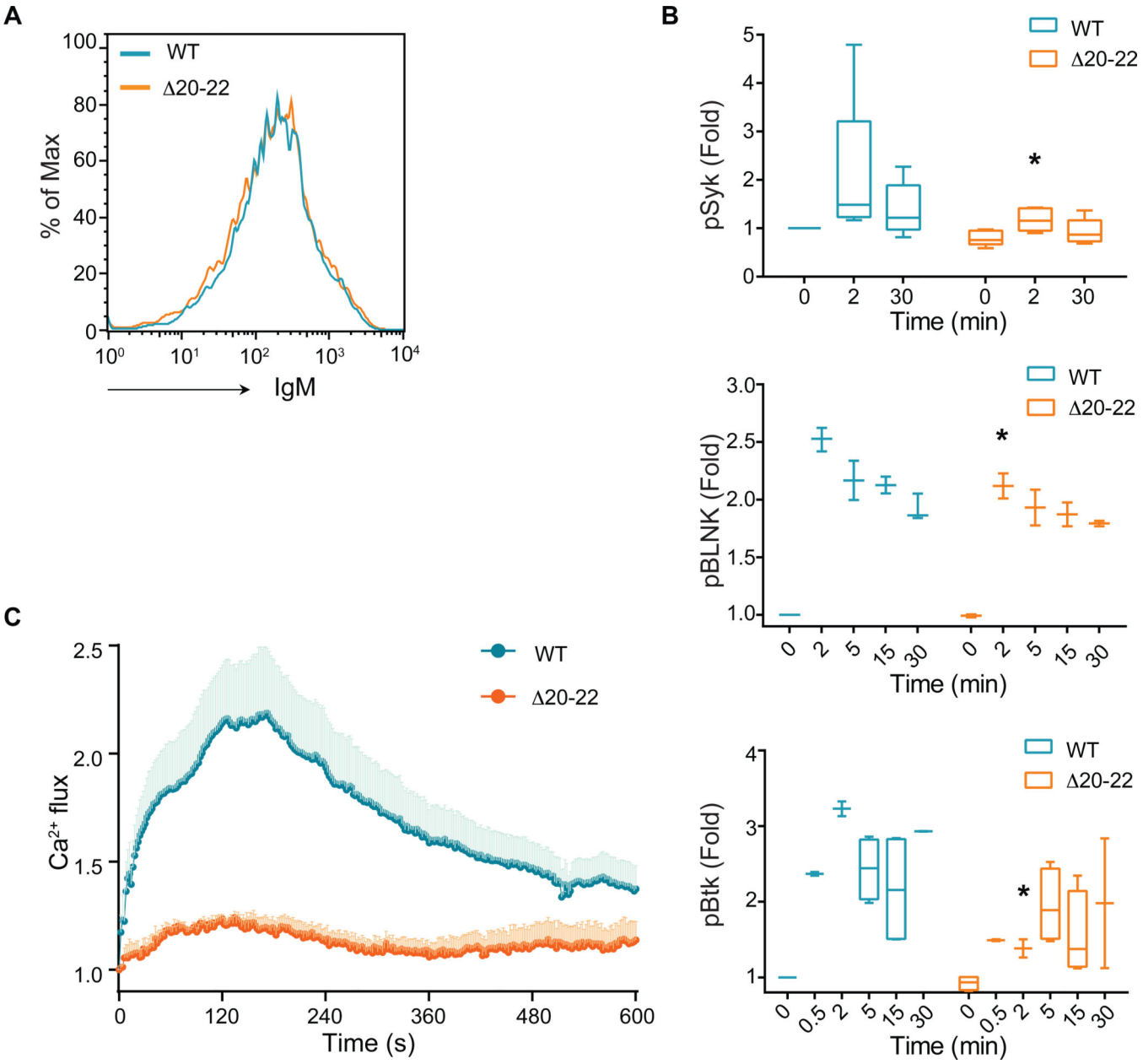

Fig. 4. The transient expression of Δ20–22 PLC-γ2 in B cells from healthy donors recapitulates the signaling defects of PLAID B cells

(**A**) B cells transiently transfected with plasmids encoding either WT PLC-γ2-GFP (WT) or Δ20–22 PLC-γ2-GFP (Δ20–22) were analyzed by flow cytometry to determine the cell surface abundance of the IgM BCR. Data rea representative of three independent experiments. (**B**) B cells expressing either WT PLC-γ2-GFP or Δ20–22 PLC-γ2-GFP were stimulated with anti-IgM for the indicated times, and then the MFIs of pSyk (top), pBLNK (middle), and pBtk (bottom) in GFP^+ and IgM^+ B cells were determined by flow cytometric analysis. Graphs show Box and Whiskers plots with the median, as well as the minimum and maximum, for the fold-increase in the MFI of the indicated phosphorylated proteins at the indicated times relative to the MFI of cells expressing WT PLC-γ2-GFP at time zero. Data

are from five independent experiments for pSyk and pBtk, and three independent experiments for pBLNK. **P* < 0.05. (**C**) B cells expressing either WT PLC-γ2-GFP (n = 9) or Δ20–22 PLC-γ2-GFP (n = 4) were labeled with Fluo4, and Ca^{2+} flux in the cells was monitored by epifluorescence microscopy over time in response to incubation on anti-IgM–coated bilayers. Data are the average of the results of three independent experiments.

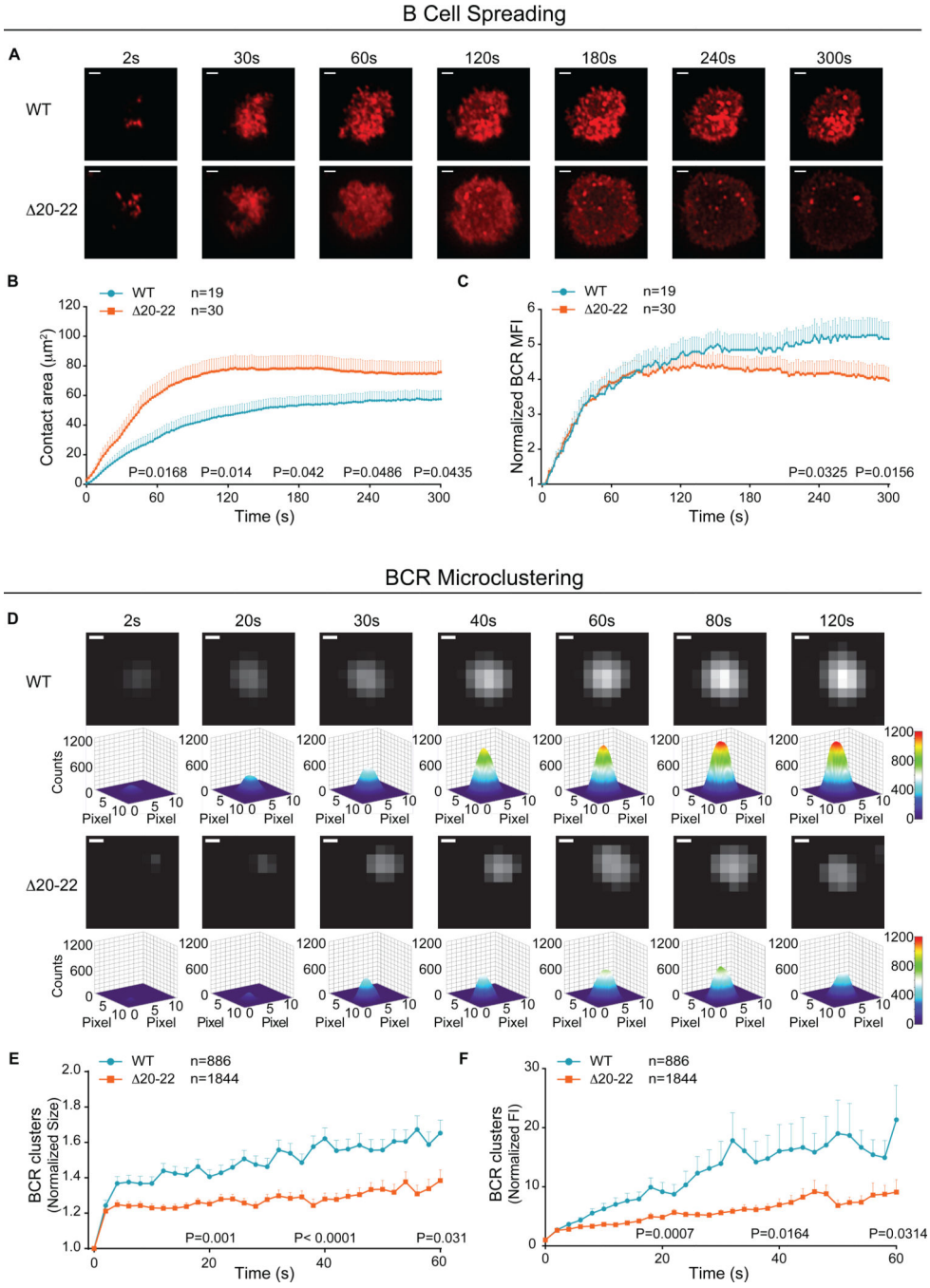

Fig. 5. The effect of the Δ20–22 PLC-γ2 variant on BCR clustering and B cell spreading

(**A**) Human peripheral B cells transiently transfected with plasmids expressing either WT PLC-γ2-GFP (top) or Δ20–22 PLC-γ2-GFP (bottom) were labeled with DyLight 649-conjugated Fab anti-IgM, placed on anti-IgM bilayers (movie S1), and imaged by TIRF microscopy. Representative time-lapse images are shown. Scale bar: 2 μm. (**B** and **C**) Quantification of (B) the size of the contact area of the indicated B cells with the lipid bilayers and (C) the normalized MFI of the BCR within the contact area over time was performed for from 19 to 30 human B cells of each type obtained from three independent

experiments. (**D**) Transfected B cells expressing either WT PLC-γ2-GFP or Δ20–22 PLC-γ2-GFP were labeled with DyLight 649-conjugated Fab anti-IgM antibody and analyzed by TIRF microscopy. Time-lapse TIRF images (see movie S2) and pseudocolored 3D surface plot images of representative BCR microclusters are shown. Individual BCR microclusters at each time point were fitted by 2D Gaussian fitter, and a 3D surface plot for each image was obtained with the ImageJ 3D surface plot plugins program. For each image, the display range is set from 0 to 1200 to enable direct comparisons to be made. Scale bar: 0.2 μm. (**E** and **F**) Quantification of (E) the sizes and (F) the normalized fluorescence intensity (FI) of all of the BCR microclusters analyzed as shown in (D) was performed. Data are means ± SEM of BCR clusters in B cells expressing either WT PLC-γ2 (n = 886 cells) or Δ20–22 PLC-γ2 (n =1844 cells) from the same images taken in (A). At the indicated times, two tailed student's *t* tests were performed for statistical comparisons, and *P* values are indicated in the plots.

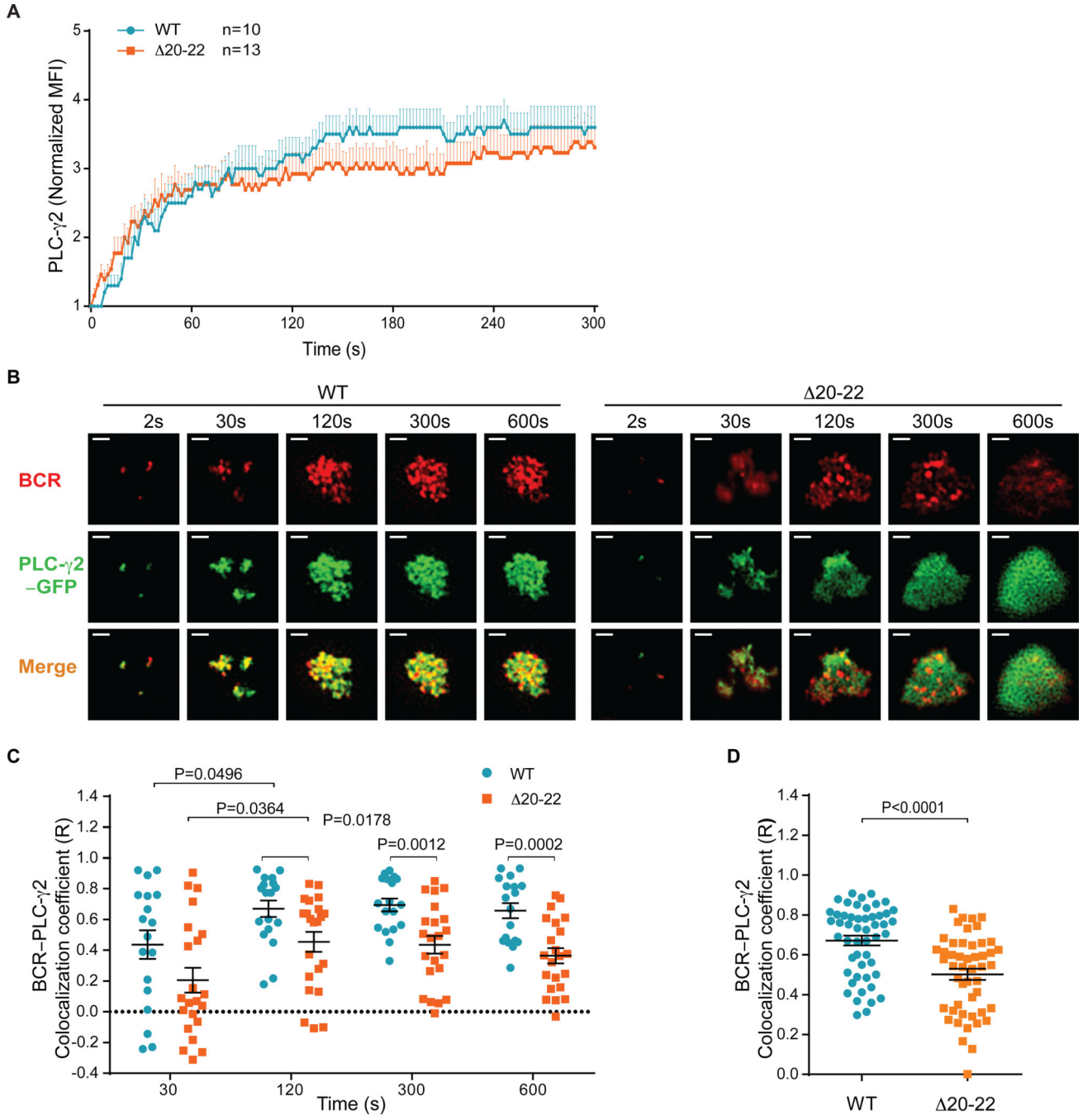

Fig. 6. The Δ20–22 PLC-γ2 variant is recruited to the plasma membrane after BCR crosslinking, but only transiently colocalizes with BCR clusters

(**A** to **D**) Human B cells transiently transfected with plasmids expressing either WT PLC-γ2-GFP or Δ20–22 PLC-γ2-GFP were placed on anti-IgM bilayers and analyzed by two-color, time-lapse TIRF microscopy over 600 s. (A) Quantification of the MFI of the PLC-γ2-GFP in the contact areas of the indicated cells over time. (B) Representative two-color, time-lapse, live-cell TIRF images (see movie S3) of B cells expressing either WT PLC-γ2-GFP (left) or Δ20–22 PLC-γ2-GFP (right). Images shown are of the BCR (red), PLC-γ2-GFP (green), and merged images. Scale bar: 2μm. (**C**) Pearson's colocalization coefficients

between BCR and PLC-γ2 in the B cells imaged in (B) were determined as described earlier. (**D**) Colocalization between BCR and PLC-γ2 in cells fixed 15 min after cells were placed on anti-IgM bilayers. Data in C and D are means ± SEM from three independent experiments. Two tailed student's *t* test or ANOVA were performed for statistical analysis and *P* values are indicated in the graphs.

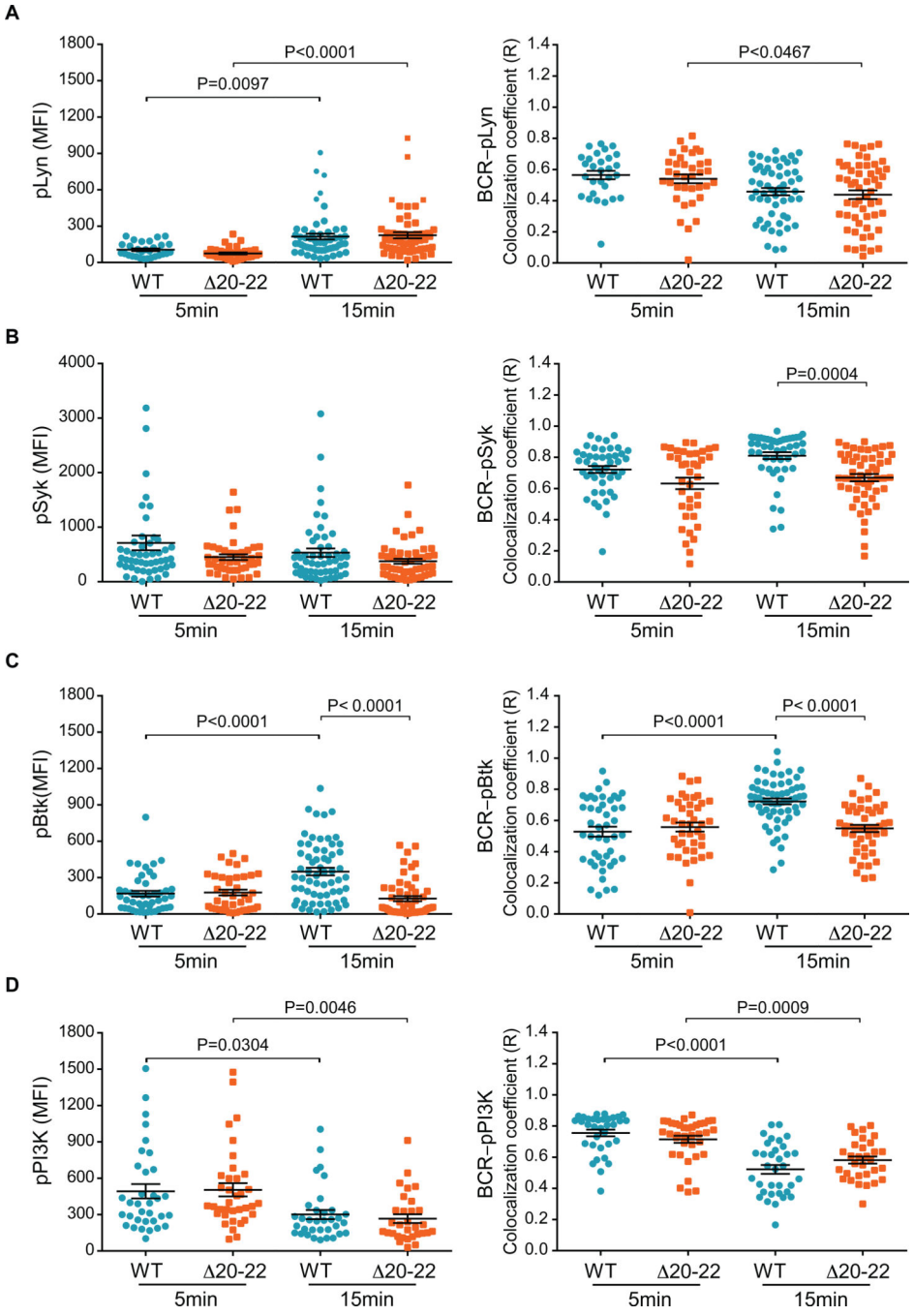

Fig. 7. The phosphorylation and colocalization of early signaling-related kinases with the BCR

(**A** to **D**) Human B cells transiently transected with plasmids expressing either WT PLC-γ2-GFP or Δ20–22 PLC-γ2-GFP were labeled with DyLight 649-Fab anti-IgM, placed on anti-IgM bilayers for 5 or 15 min, fixed, permeabilized, and stained with antibodies specific for (A) pLyn, (B) pSyk, (C) pBtk, or (D) pPI3K, and then were imaged by TIRF microscopy. Left: The MFIs of (A) pLyn, (B) pSyk, (C) pBtk, and (D) pPI3K. Right: The Pearson's colocalization coefficients (R) between the BCR and (A) pLyn, (B) pSyk, (C) pBtk, and (D) pPI3K were determined as described earlier. Each data point represents the value obtained

from an individual cell analyzed in a single independent experiment. Data are means ± SEM from three independent experiments. *P* values were calculated by ANOVA analysis.

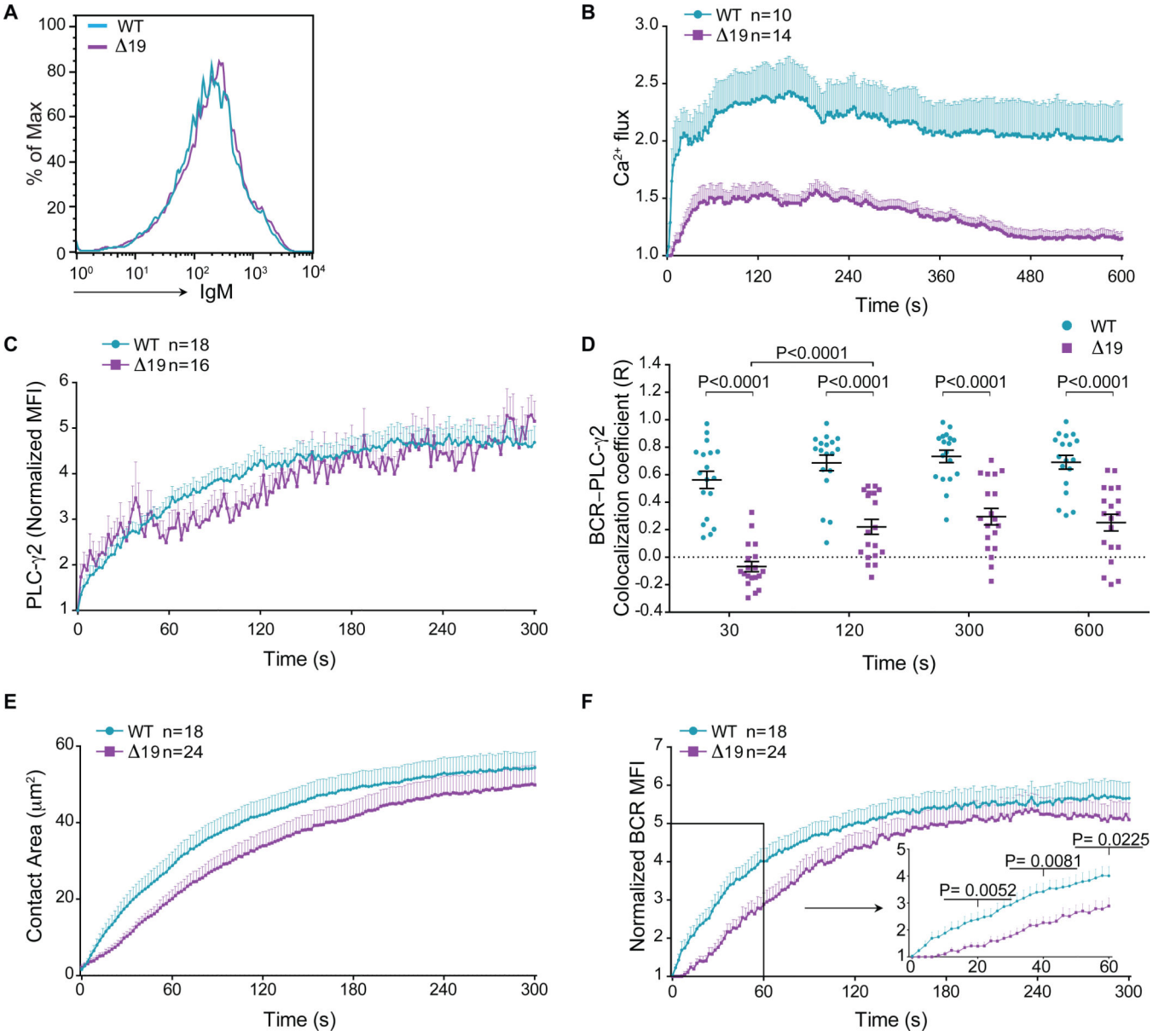

Fig. 8. BCR signaling defects in HC donor B cells expressing the Δ19 PLC-γ2 variant are similar to those in HC donor B cells expressing the Δ20–22 PLC-γ2 variant

(**A**) B cells transfected with plasmids expressing either WT PLCγ2-GFP or Δ19 PLCγ2-GFP were analyzed by flow cytometry to determine the cell surface abundance of the BCR. Flow cytometry profiles are representative of three independent experiments. (**B**) B cells transfected with plasmid expressing either WT PLCγ2-GFP or Δ19 PLCγ2-GFP were incubated on anti-IgM–coated bilayers, and Ca^{2+} flux in the cells was monitored as described earlier. Data are means ± SEM from 10 (WT) and 14 (Δ19) cells. (**C** to **F**) B cells transfected with plasmids expressing either WT PLC-γ2-GFP or Δ19 PLC-γ2-GFP were placed on anti-IgM bilayers and analyzed by time-lapse, live-cell TIRF microscopy. (C) Quantification of the MFI of the PLC-γ2-GFP in the contact area of the indicated B cells over time. Data are means ± SEM from 18 (WT) and 16 (Δ19) cells. (D) Pearson's

colocalization coefficients between BCR and PLC-γ2 in the indicated cells over time were determined. Data are means ± SEM from 18 (WT) and 19 (Δ19) cells. Each data point represents the value obtained from a single cell analyzed in one of three independent experiments. Statistical significance was determined by ANOVA. Quantification of (E) the size of the contact area and (F) the normalized MFI of the BCR within the contact area. Data are means ± SEM from 18 (WT) and 24 (Δ19) cells. Two tailed student's *t* tests were performed for statistical comparisons, and *P* values are provided at the indicated times in the inset.

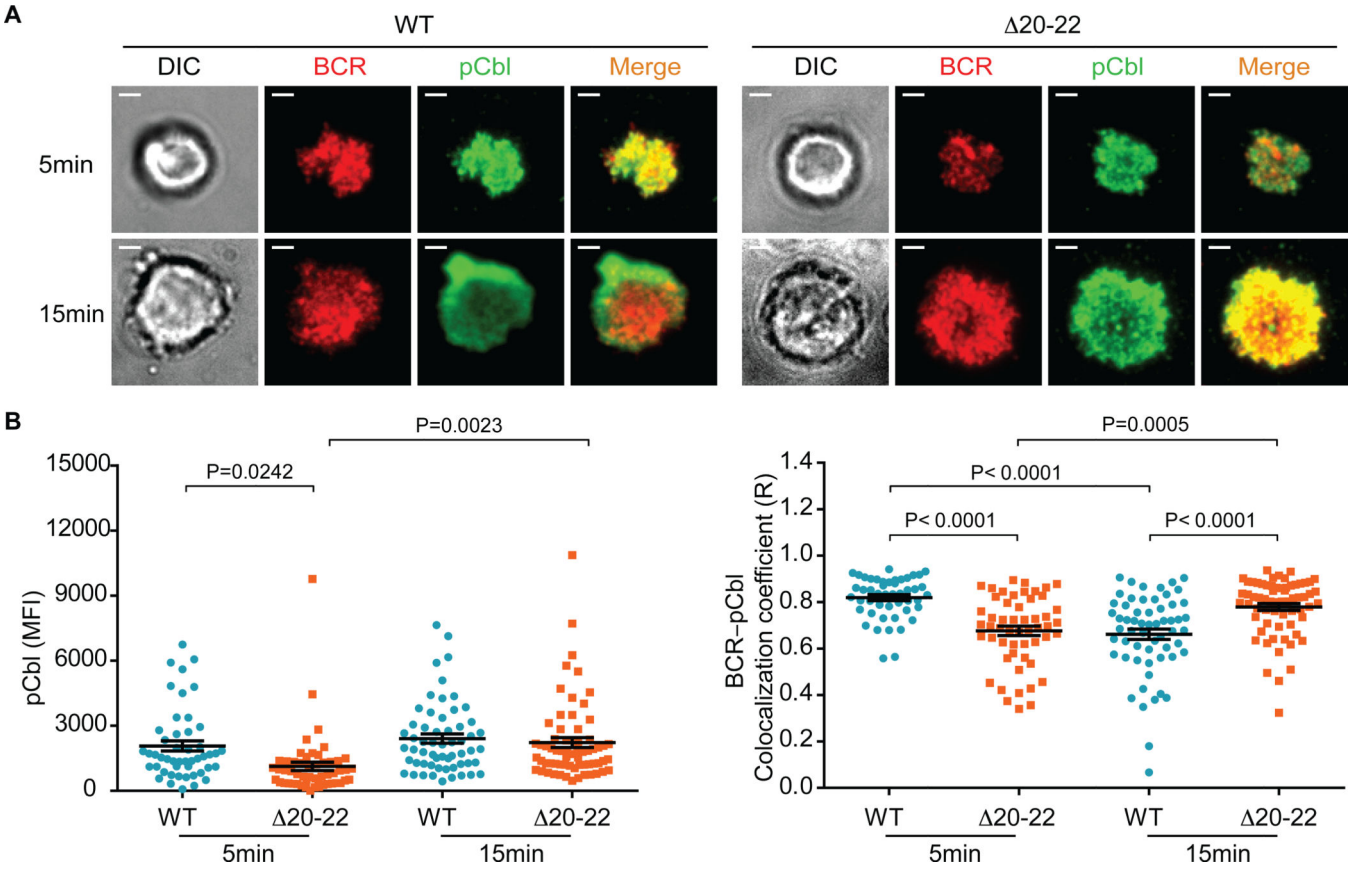

Fig. 9. Spatial and temporal dysregulation of pCbl in B cells expressing the Δ20–22 variant PLC-γ2-GFP

(**A** and **B**) Human B cells transfected with plasmids expressing either WT PLC-γ2-GFP or Δ20–22 PLC-γ2-GFP were labeled with DyLight 649-Fab anti-IgM, placed on anti-IgM bilayers for 5 or 15 min, fixed, stained with antibody specific for pCbl (Tyr^{700}), and imaged by TIRF microscopy. (A) Representative TIRF images for the BCR (red) and pCbl (green), as well as merged images are shown. (B) Left: Means ± SEM of the MFI of pCbl. Right: Pearson's colocalization coefficients for the BCR and pCbl. Each data point represents the values from a cell analyzed in one of two independent experiments. Statistical analysis was performed by ANOVA.